NASA TECHNICAL MEMORANDUM

NASA TM X-72834

NASA TM X-72834

(NASA-TM-X-72834) MEASUREMENTS OF WAVE HEIGHT STATISTICS AND RADAR, CROSS-SECTION IN A WIND WAVE TANK (NASA) 21 p HC $3.50
CSCL 17I

N76-22422

Unclas
G3/32 26880

MEASUREMENTS OF WAVE HEIGHT STATISTICS AND RADAR CROSS-SECTION IN A WIND WAVE TANK

J. W. Johnson
A. E. Cross

March 5, 1976

NATIONAL AERONAUTICS AND SPACE ADMINISTRATION
LANGLEY RESEARCH CENTER, HAMPTON, VIRGINIA 23665

1. Report No.	2. Government Accession No.	3. Recipient's Catalog No.
NASA TM X-72834		

4. Title and Subtitle	5. Report Date
Measurements of Wave Height Statistics and Radar Cross-Section in a Wind Wave Tank	April 1976
	6. Performing Organization Code
7. Author(s)	8. Performing Organization Report No.
J. W. Johnson, A. E. Cross	
	10. Work Unit No.
9. Performing Organization Name and Address	
NASA Langley Research Center Hampton, Virginia 23665	11. Contract or Grant No.
	13. Type of Report and Period Covered
12. Sponsoring Agency Name and Address	NASA Technical Memorandum
National Aeronautics & Space Administration Washington, D. C. 20546	14. Sponsoring Agency Code

15. Supplementary Notes

16. Abstract

There is currently wide interest among oceanographers and meteorologists in remote sensing of ocean surface characteristics. A wind wave tank developed at Langley Research Center is being used to evaluate various remote sensing techniques based on electromagnetic scattering phenomena, and in the development and evaluation of theoretical scattering models. This paper describes the wave tank, documents the statistics of the rough water surface, and presents microwave radar cross-section measurement results. The water surface statistics are similar in key respects to the open ocean and the microwave scattering measurements show, qualitatively, theoretically predicted large and small scale scattering effects.

17. Key Words (Suggested by Author(s)) (STAR category underlined)	18. Distribution Statement
Wind waves Wave tank Electromagnetic scattering Rough surface scattering Radar cross section Radio oceanography	UNCLASSIFIED - UNLIMITED

19. Security Classif. (of this report)	20. Security Classif. (of this page)	21. No. of Pages	22. Price*
UNCLASSIFIED	UNCLASSIFIED	19	$3.25

* For sale by the National Technical Information Service, Springfield, Virginia 22161

INTRODUCTION

There is currently wide interest among oceanographers and meteorologists in the developing technology for remote sensing of ocean surface characteristics. An airborne or satellite-borne microwave radar system offers an efficient means of providing global maps of ocean roughness properties and surface wind fields. A wind wave tank was developed at Langley Research Center to investigate electromagnetic scattering from wind driven, rough water surfaces in support of on-going aircraft and satellite programs. Currently this wave tank is being used to evaluate various remote sensing techniques based on scattering phenomena, and in the development and evaluation of theoretical scattering models.

This paper describes the wind wave system, documents the statistical properties of the rough water surface as measured with a resistive wave staff, and presents the results of measurements of the average scattering cross-section of the water surface with a 24 GHz microwave scatterometer.

Wind speeds of 0-25 knots (12.5 m/sec.) generated 0.8 cm maximum rms wave heights in the tank. Probability density histograms and power spectral density plots have been computed from temporal wave height measurements, and the results agree with open ocean measurements in key respects. The results of the microwave scattering measurements show, qualitatively, the behavior predicted by both large and small scale scattering theory.

WIND WAVE TANK DESCRIPTION

The wind wave tank consists of a water tank section, a wind diffuser section and a matched pair of adjacent blowers. The water tank is 4.9 m

long and 1.2 m wide with a mean water depth of 15 cm. A beach section 0.5 m from the downstream end of the water tank and with a slope of 1/6 minimizes standing wave patterns due to reflected waves. Water flowing over the beach goes into a trough and is recirculated to maintain a constant mean water level. A 0.8 m wide Plexiglas section in the center of the water tank is an observation area used for making optical measurements. Figure 1 shows the mid-section and downwind end of the water tank with the resistive wave staff mounted in position. The vertical structure at the far end was used for positioning and pointing the 24 GHz radar which is discussed in a later section.

Figure 2 shows the blowers and the diffuser section which were designed to give a constant and laterally uniform wind field. The diffuser is 2.6 m long with three screen baffles spaced 0.6 m apart. Direct drive blowers were required to provide a high volume, steady air flow. Wind speed was regulated using shutters at the blower exits.

WATER SURFACE STATISTICAL PROPERTIES

Surface elevation statistics, including the mean and variance along with histograms and power spectral density (PSD) plots, were measured using the resistive wave staff mentioned. The wind wave response curve is shown in Figure 3. The maximum attainable wind speed of 25 knots, measured 1.2 m down wind from the diffuser exit, produced 0.8 cm rms wave heights. Surface fluctuations generated at wind speeds less than 6 knots were beyond the resolution capability of the wave staff. The hump in the curve is a repeatable characteristic of this particular wind wave system but it is of no significance in the discussion here. Wave height probability density histograms

for wind speeds of 6, 18 and 25 knots are shown in Figures 4, 5 and 6 respectively. The wave heights are Gaussian distributed with a mean value and degree of skewness that increase with wind speed. These characteristics are consistent with open ocean conditions. Figures 7 and 8 are PSD's for 25 and 6 knot winds respectively. With 25 knot winds there is a well defined spectral peak at 2.5 Hz (observed water wave lengths of approximately 20 cm). This spectral peak becomes less dominant and shifts toward shorter wave lengths with decreasing wind speed. Like ocean waves, the high frequency region of the spectrum exhibits an f^{-5} decay, where f is frequency. At 6 knots, the spectral energy is more distributed with no dominant peak.

MICROWAVE BACKSCATTER MEASUREMENTS

A microwave radar scatterometer was used with the wave tank to investigate electromagnetic scattering from a water surface with both large and small scale roughness properties. The scattered power, P_R, was measured as a function of wind speed and scatterometer viewing angle, and the normalized radar cross section was calculated using the familiar radar equation,

$$\frac{P_R}{P_T} = \frac{G^2 \lambda^2}{(4\pi)^3 R^4} \sigma$$

where,

P_T = transmitted power

G = Antenna gain

λ = wavelength

R = range

σ = radar cross section

The normalized radar cross section, σ^o, is given by

$$\sigma^o \simeq \frac{4\pi^2 R^2 V_B^2 \cos\theta}{\lambda^2} \cdot \frac{P_R}{P_T}$$

after making the substitutions,

$$\sigma = \sigma^o A$$

and

$$G \simeq \frac{4}{V_B^2}$$

where

A = illuminated area

V_B = antenna 3 dB beam width

θ = incidence angle

This approximation to the antenna gain is a result of considering the gain function to be unity within the 3 dB points and zero elsewhere.

There are two separate scattering mechanisms involved in theoretically modeling the rough water surface. Specular scattering due to the large scale roughness, where the water wavelength is much greater than the electromagnetic wavelength, can be modeled in terms of the wave slope statistics. Both the horizontally and vertically polarized cross sections, $\sigma^o_{hh} = \sigma^o_{vv}$ respectively, are given by

$$\sigma^o_{hh} = \sigma^o_{vv} = \frac{\pi}{\cos^4\theta} p(\tan\alpha)$$

where $p(\tan \alpha)$ is the probability density function of the slopes of the large scale waves. Gravity is the restoring force for waves that normally fall into the large scale class; thus, the term gravity waves is commonly used. In addition, wind generated waves consist of small ripples, or capillary waves whose restoring force is surface tension, superimposed on the large scale structure. These waves present a slightly rough surface, characterized by water wave lengths on the order of the electromagnetic wavelength, that is modeled in terms of the height statistics of the waves. The horizontally and vertically polarized cross sections for a slightly rough surface are given by

$$\sigma^o_{hh} = 4 \pi k_o^4 \cos^4\theta \; S(2k_o \sin\theta)$$

$$\sigma^o_{vv} = 4 \pi k_o^4 (1 + \sin^2\theta)^2 \; S(2k_o \sin\theta)$$

where $S(2k_o \sin\theta)$ is the height spectrum of the capillary waves and $k_o = 2\pi / \lambda$. Figure 9 is an example of computed results using a composite (large and small scale) model to calculate normalized radar cross-section as a function of viewing angle. For shallow angles near nadir, specular scattering is the dominant mechanism and there is no polarization dependence. However, for angles greater than 25^o resonant scattering from the small scale structure dominates. There is a polarization dependence, and for vertical polarization the scattering is quite diffuse.

The 24 GHz, homodyne radar in Figure 10 (block diagram in Figure 11) was used to investigate basic microwave scattering phenomena in the wind wave tank. The radar was positioned approximately 1.8 m from the water surface, thus illuminating a 0.76 m diameter spot. The average

scattered power was measured for the full range of wind speeds and for viewing angles out to 60^{o}. The results for vertical polarization are shown in Figure 12. For shallow angles, the specular scattering becomes more diffuse as the surface is roughened by increasing wind speed and the return signal at a given incidence angle diminishes. The results at low wind speeds are inconclusive since the water wave spectra show that there are no dominant large scale waves; thus, the frequency of the specular component of the scattered energy would have zero doppler shift. Consequently, the specular component at low wind speeds was not detectable using a homodyne scatterometer. The σ^{o} polarization dependence predicted by the small scale scattering theory was observed as shown in Figure 13.

CONCLUDING REMARKS

A wind wave tank capable of generating 0.8 cm rms wave heights with 25 knot winds was developed and its performance evaluated at LaRC. Experimental results have been presented defining the statistical properties of the rough water surface at the various wind speeds, and microwave measurement results demonstrate that the wave tank is a useful laboratory tool for investigating electromagnetic scattering from rough water surfaces. The water surface statistics show key similarities to waves in the open ocean and the microwave scattering results agree qualitatively with theoretical predictions. The wind wave tank is currently being used in on-going programs for the development of airborne and satellite-borne remote sensing techniques.

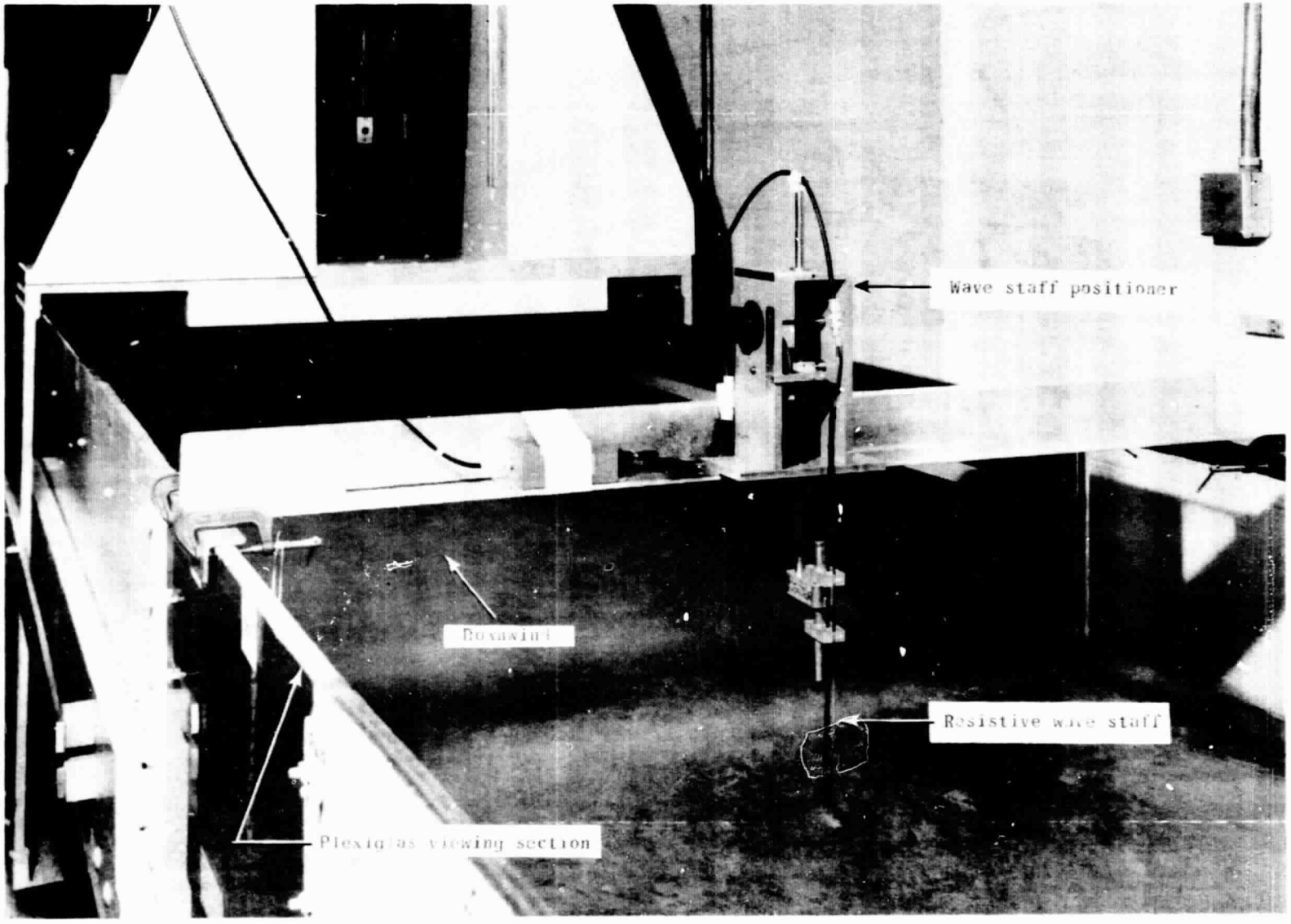

Figure 1.-Wind wave tank mid-section view with resistive wave-staff mounted for measurements.

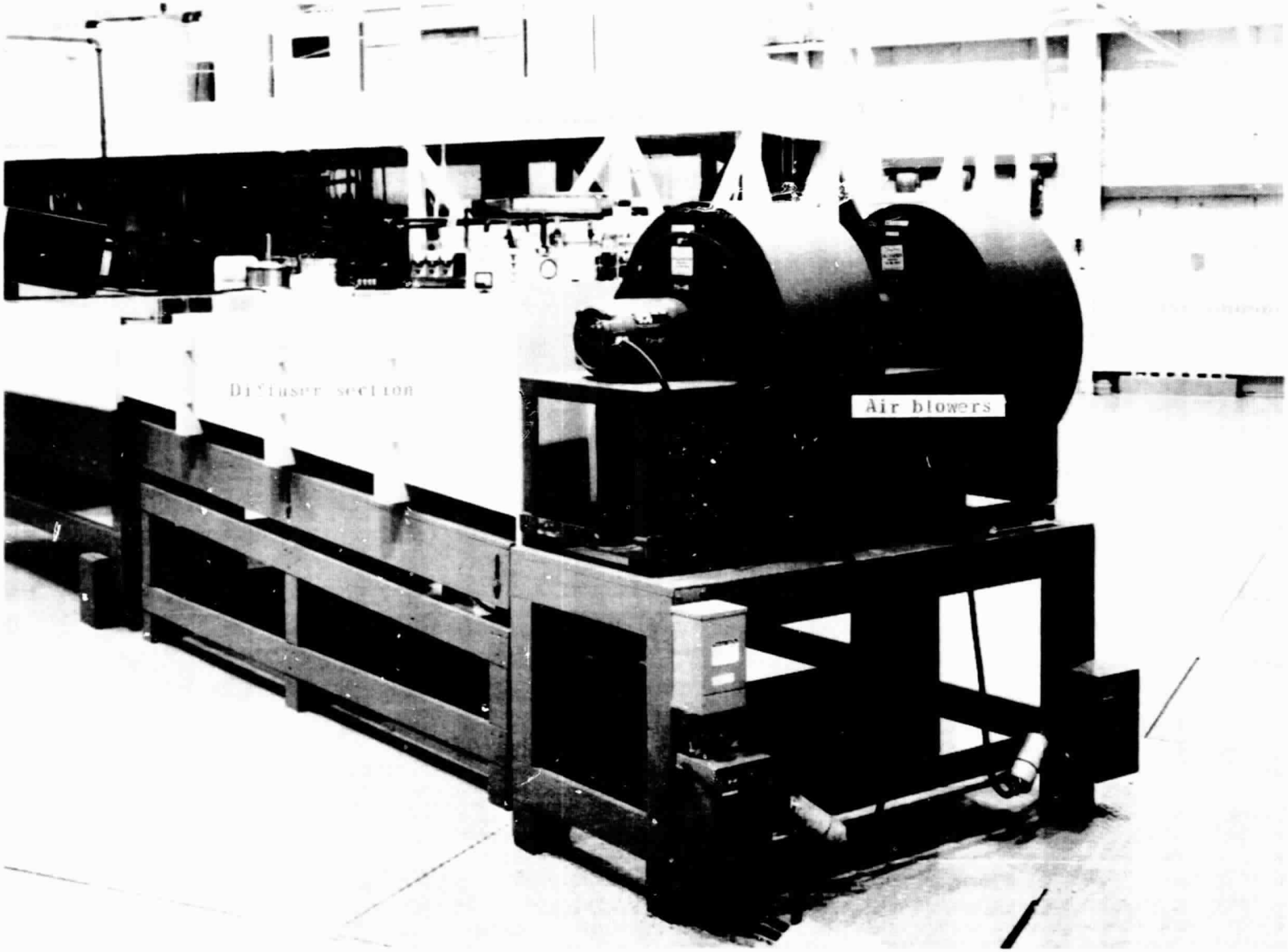

Figure 2.-View of wind wave tank showing blowers and diffuser section.

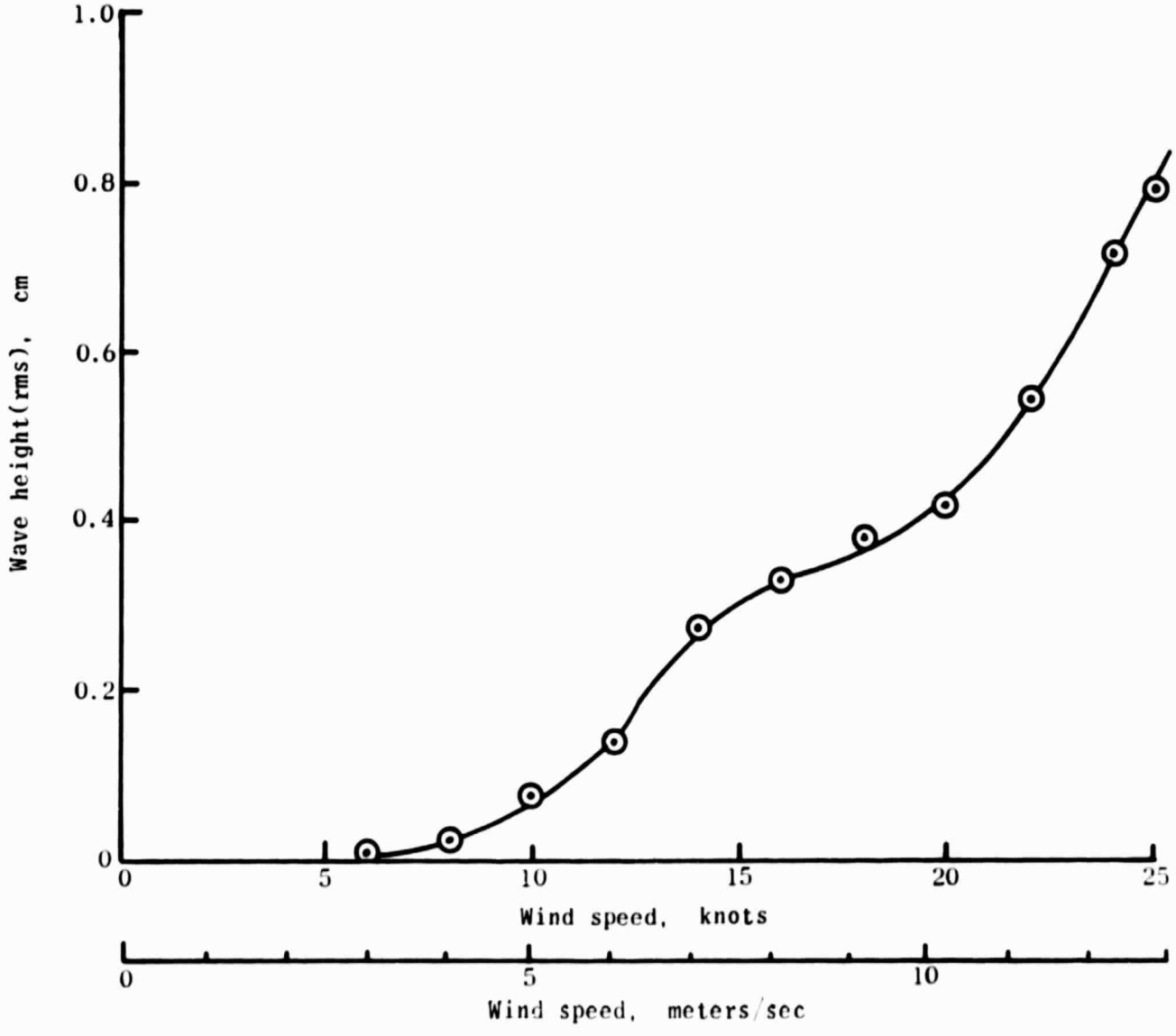

Figure 3.-Wind wave response curve for wind wave tank showing rms wave height as a function of wind speed.

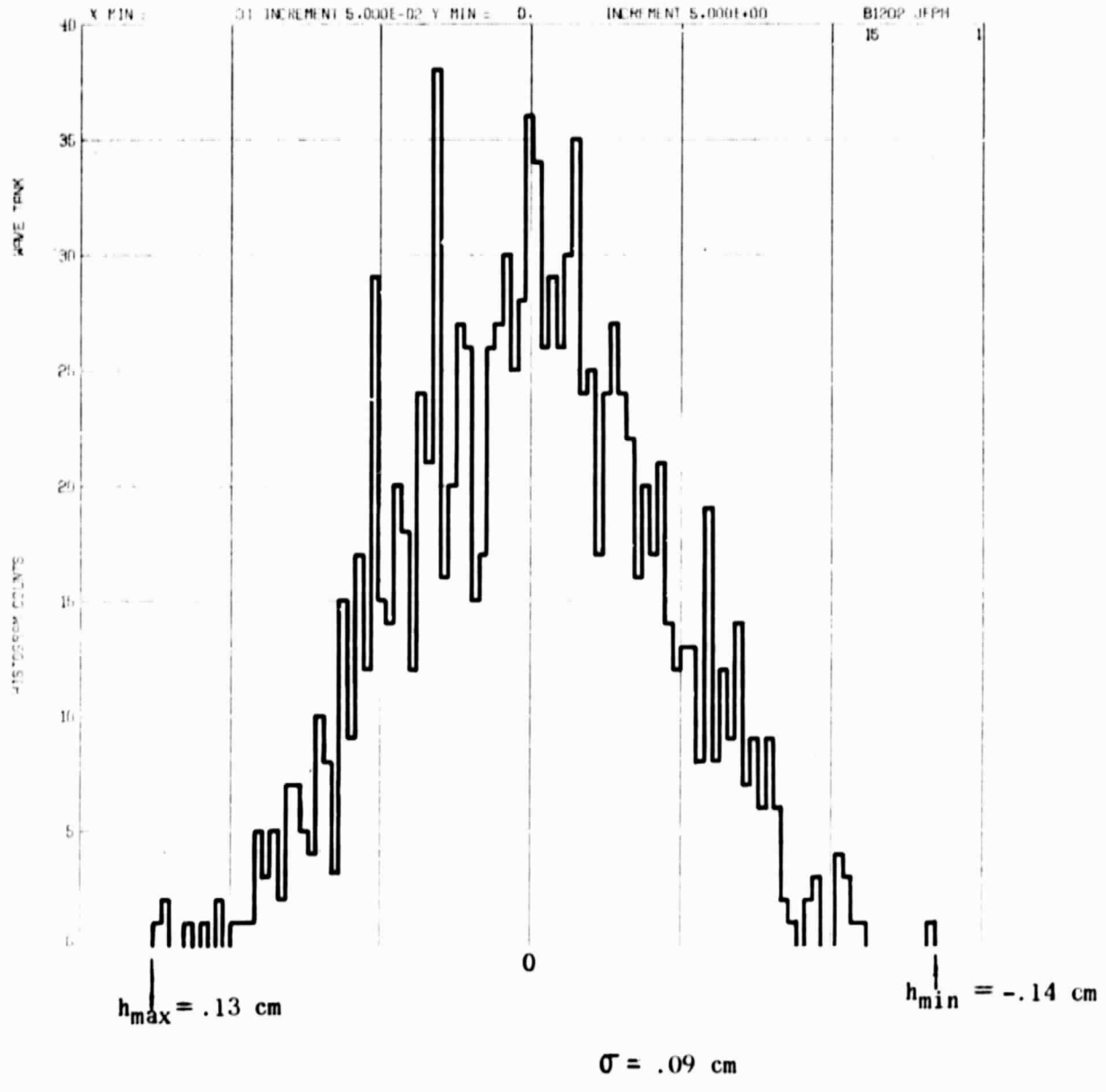

Figure 4.-Wave height probability density histogram for wind speed of 3.09 m/sec(6 knots).

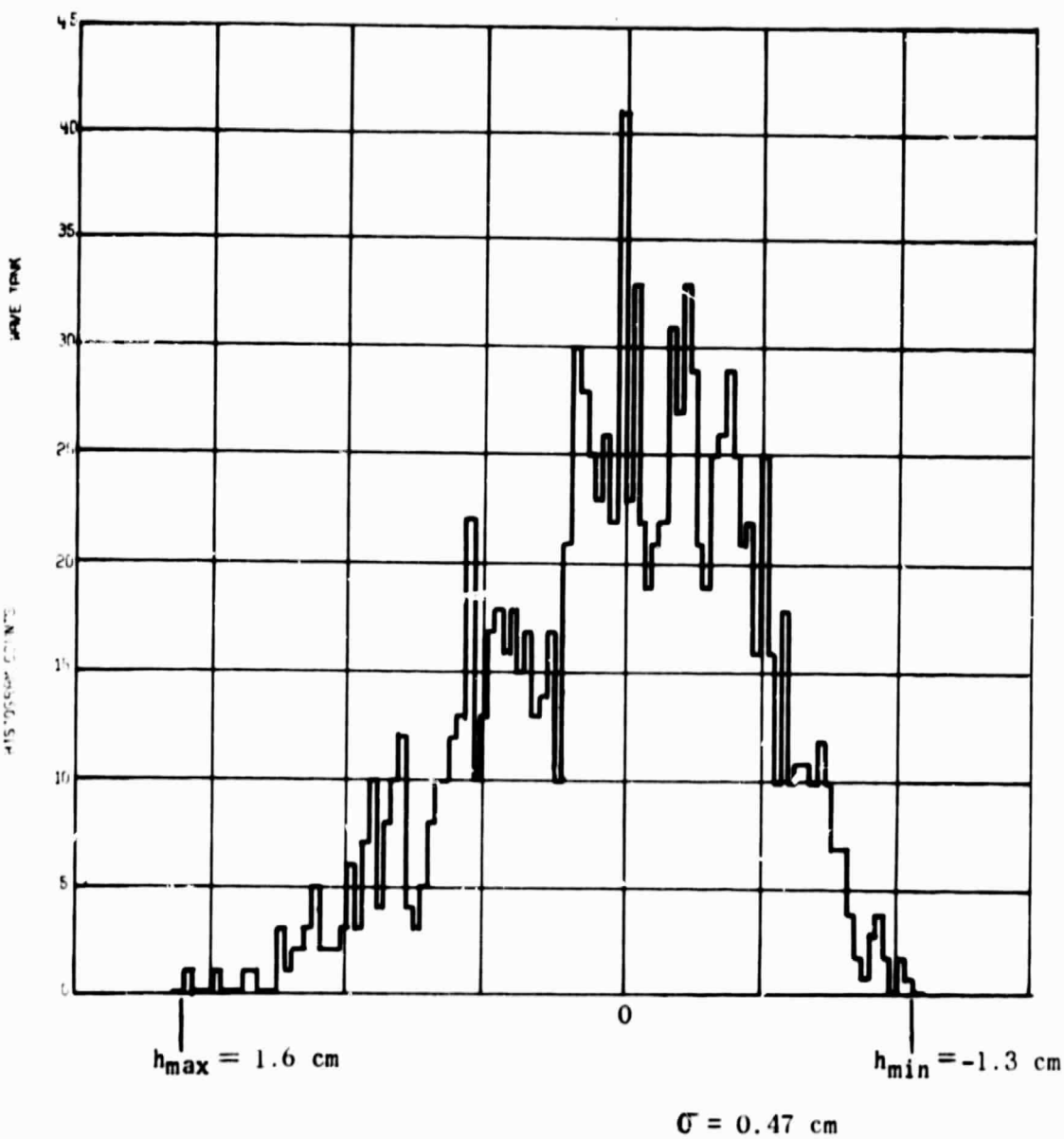

Figure 5.-Wave height probability density histogram for wind speed of 9.26 m/sec(18 knots).

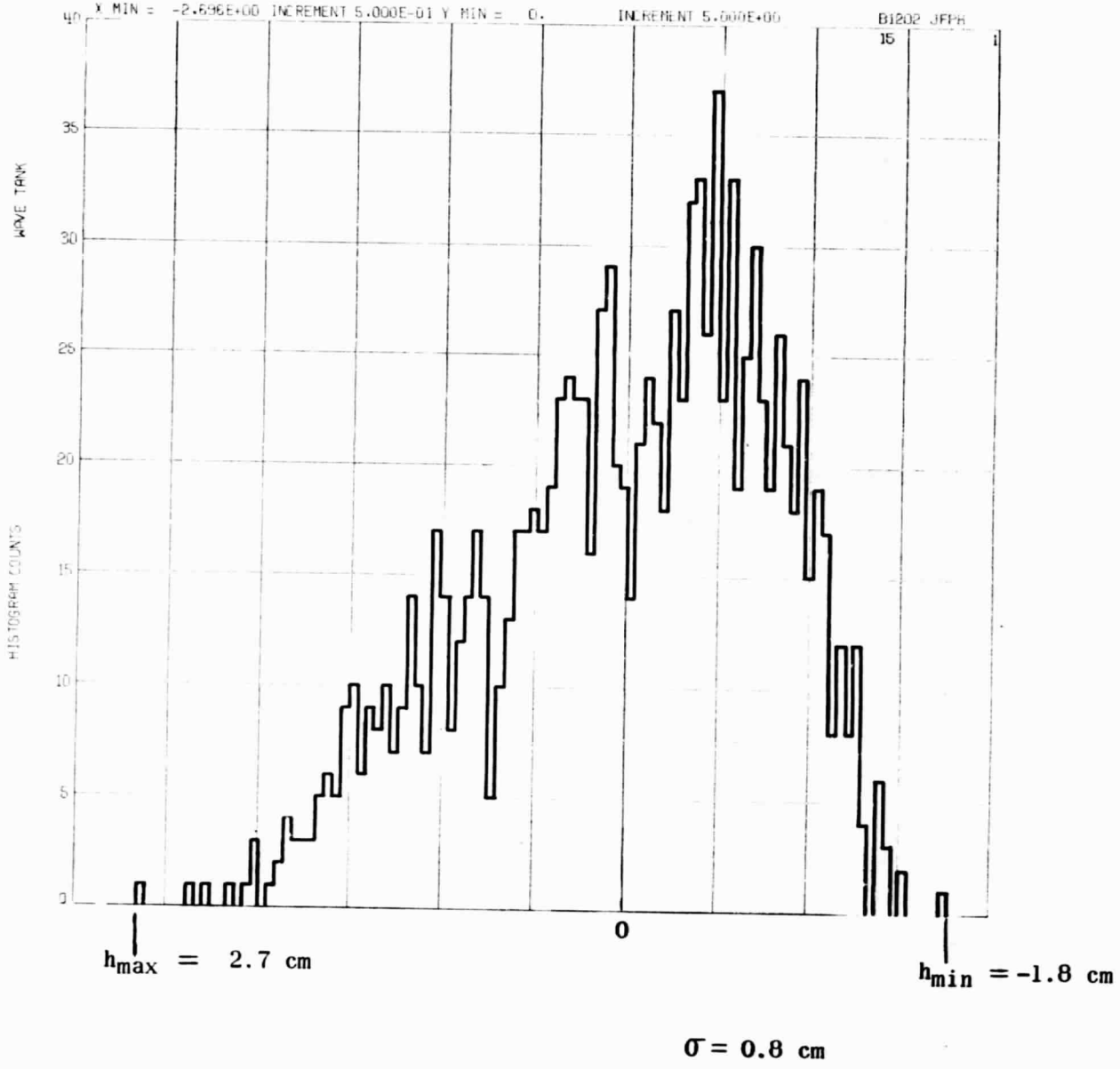

Figure 6.–Wave height probability density histogram for wind speed of 12.86 m/sec(25 knots).

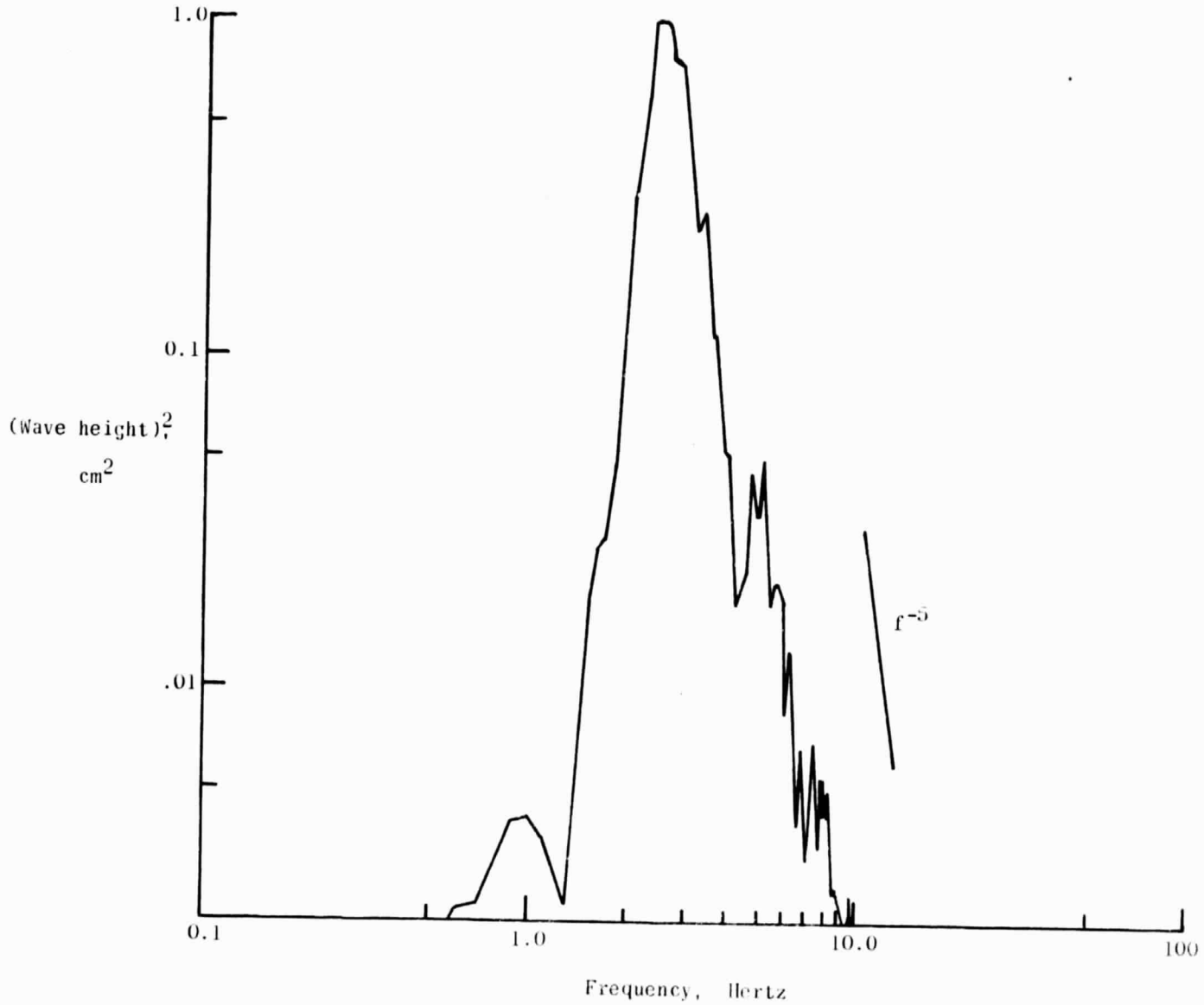

Figure 7.-Wave height power-spectral-density (PSD) for wind speed of 12.86 m/sec(25 knots).

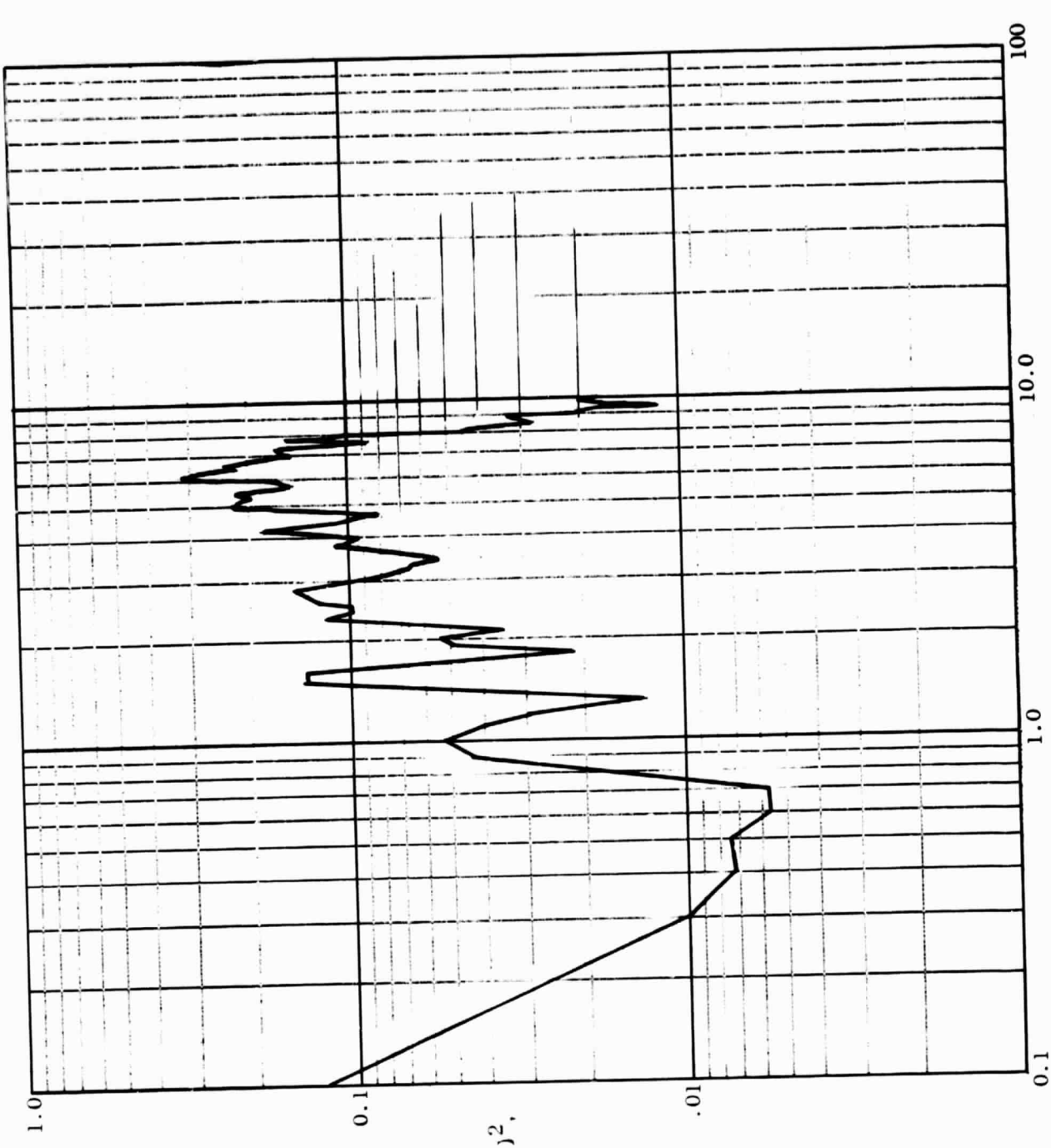

Figure 8.-Wave height power-spectral-density (PSD) for wind speed of 3.09 m/sec(6 knots

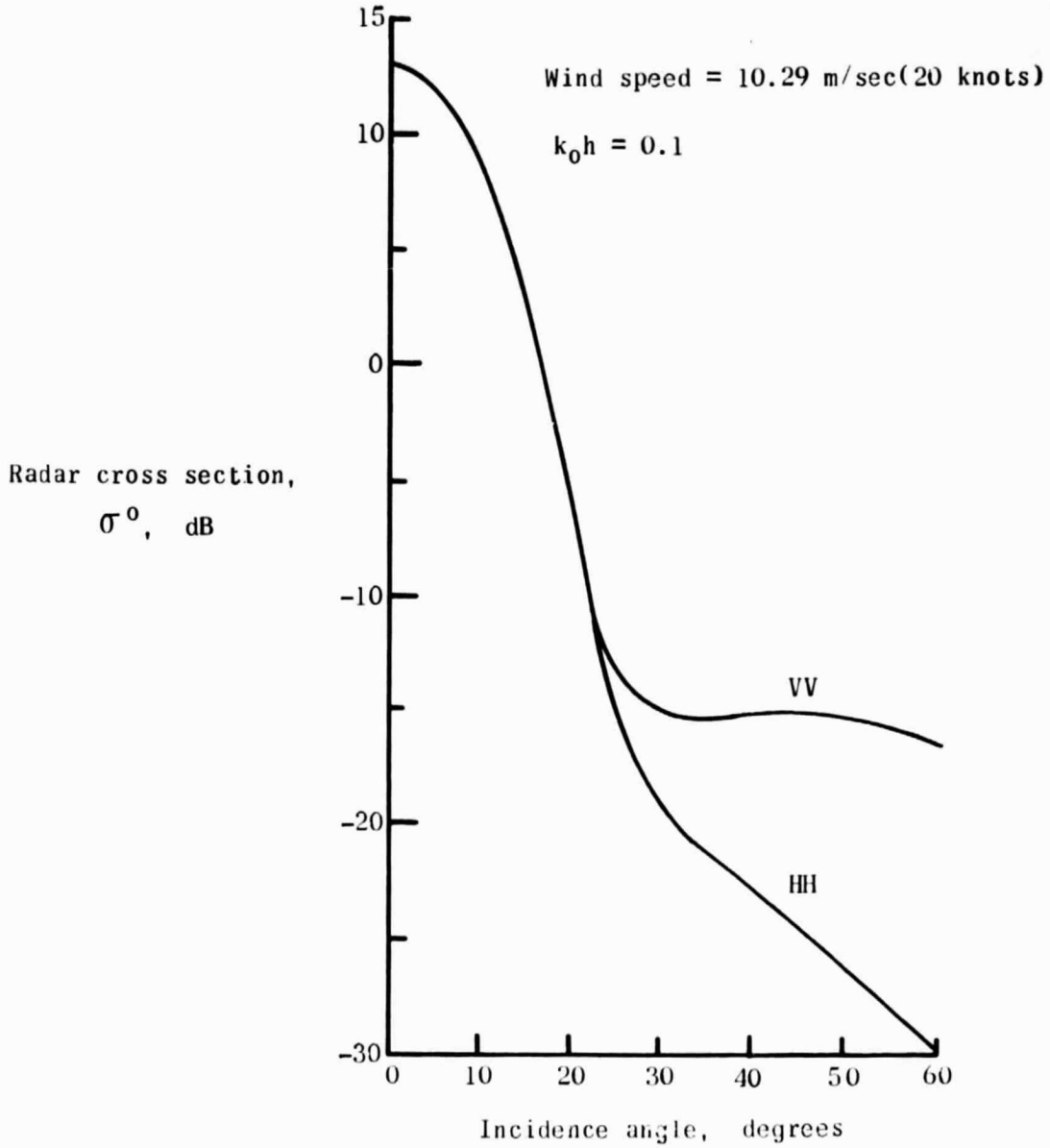

Figure 9.- Theoretical radar cross section as a function of viewing angle.

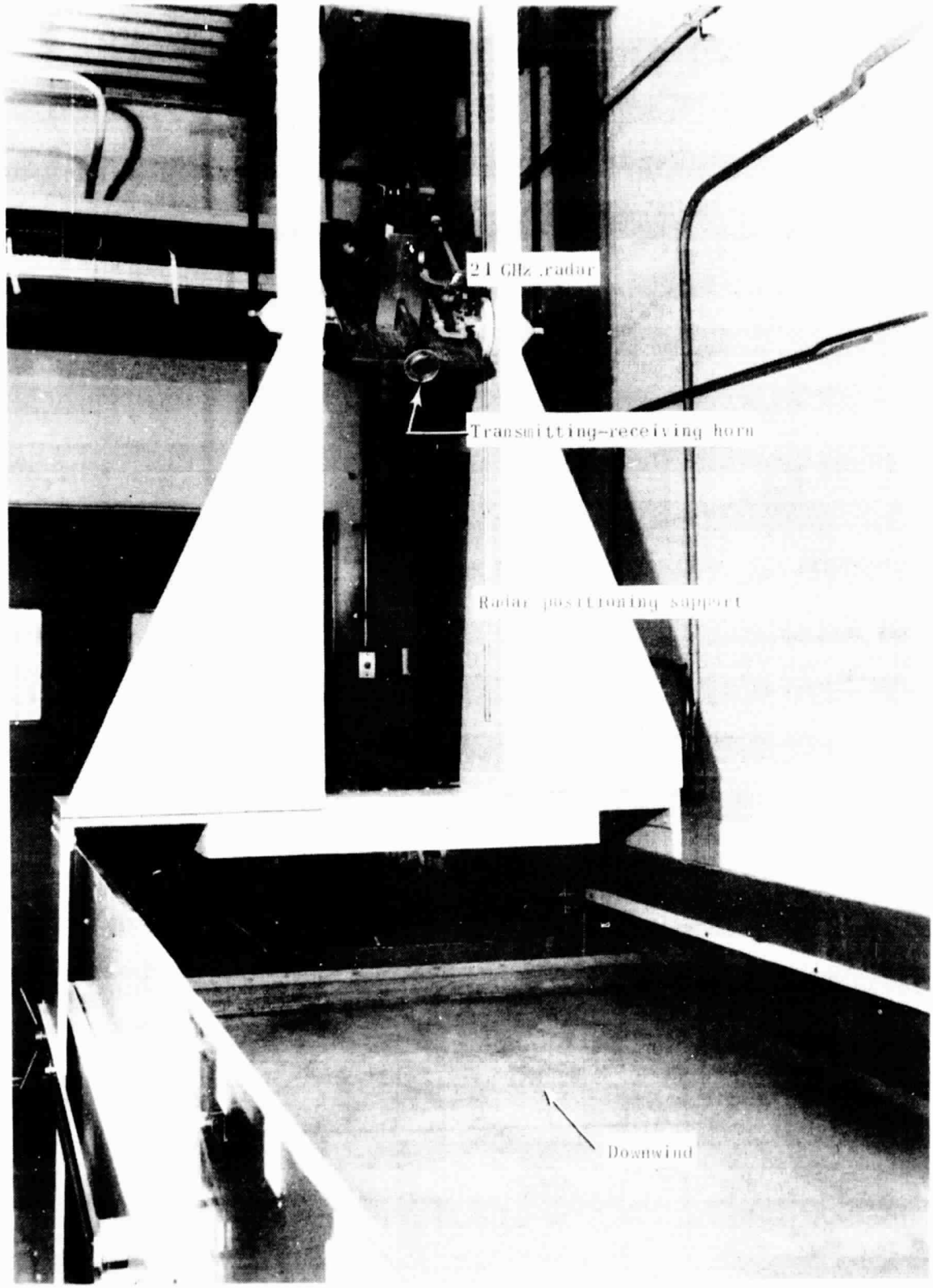

Figure 10.—Photograph of 21 GHz homodyne radar mounted in position for backscatter measurements.

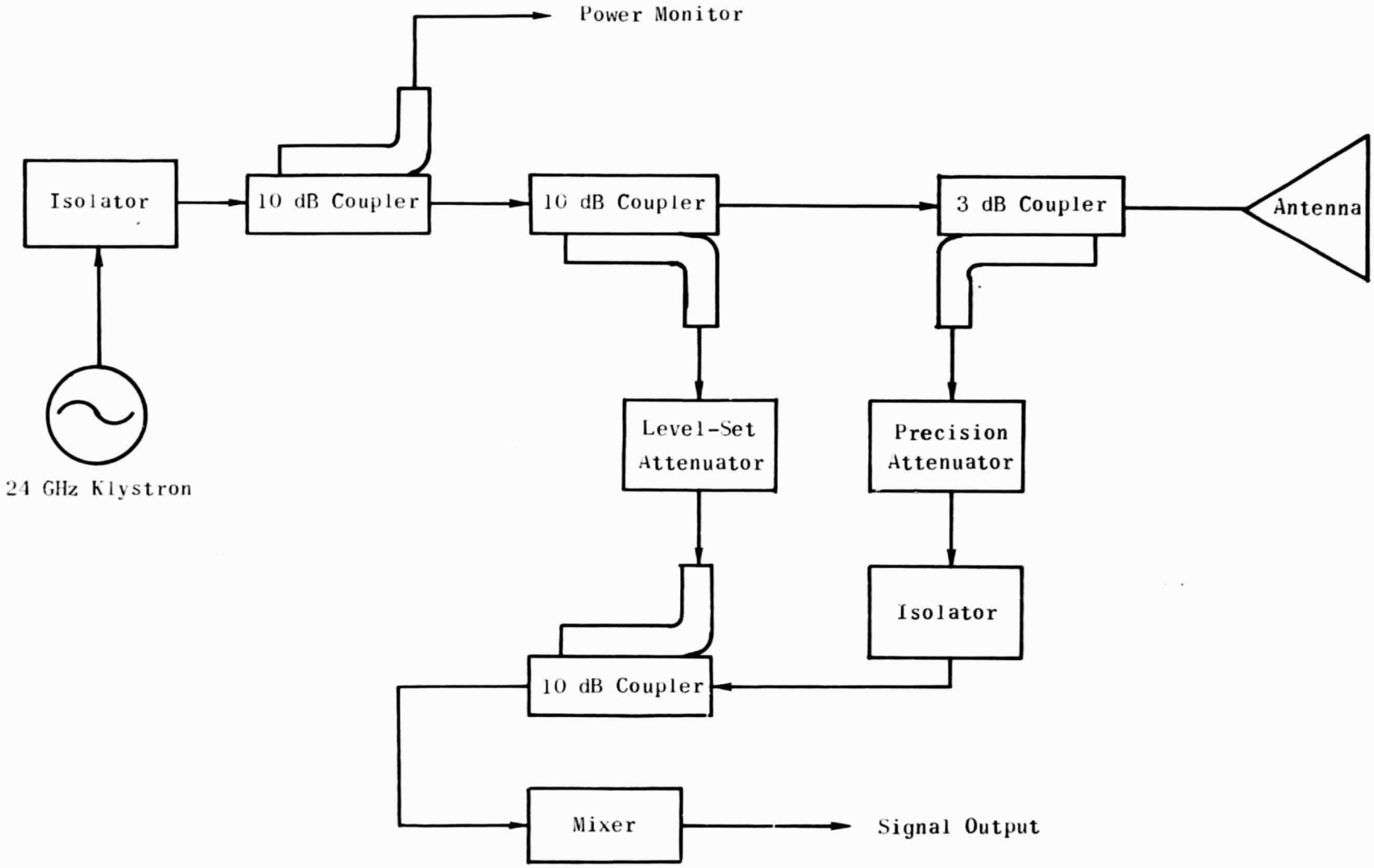

Figure 11.-Block diagram of 24 GHz homodyne radar.

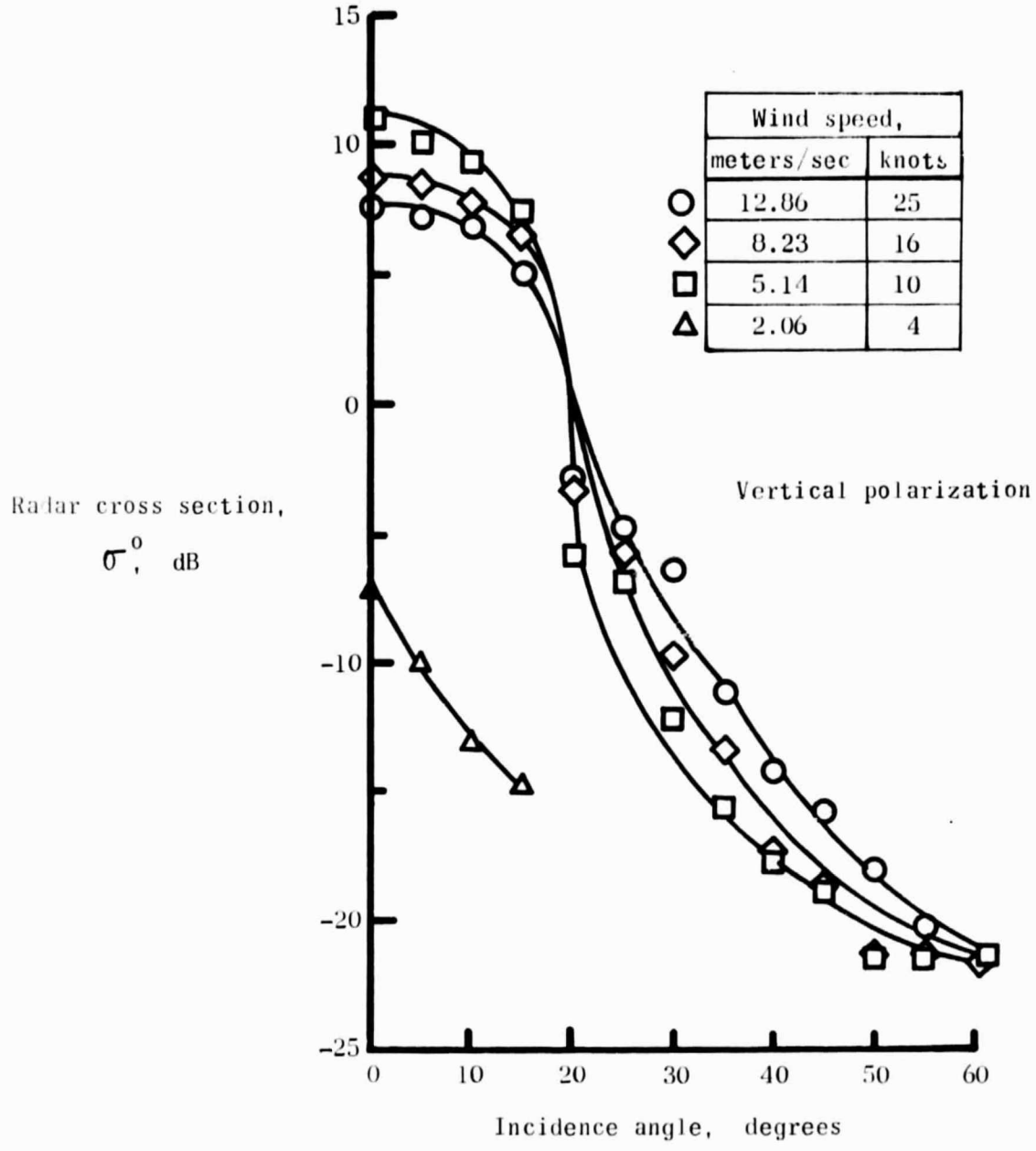

Figure 12.-Radar cross section as a function of wind speed for viewing angles from 0^0 to 60^0.

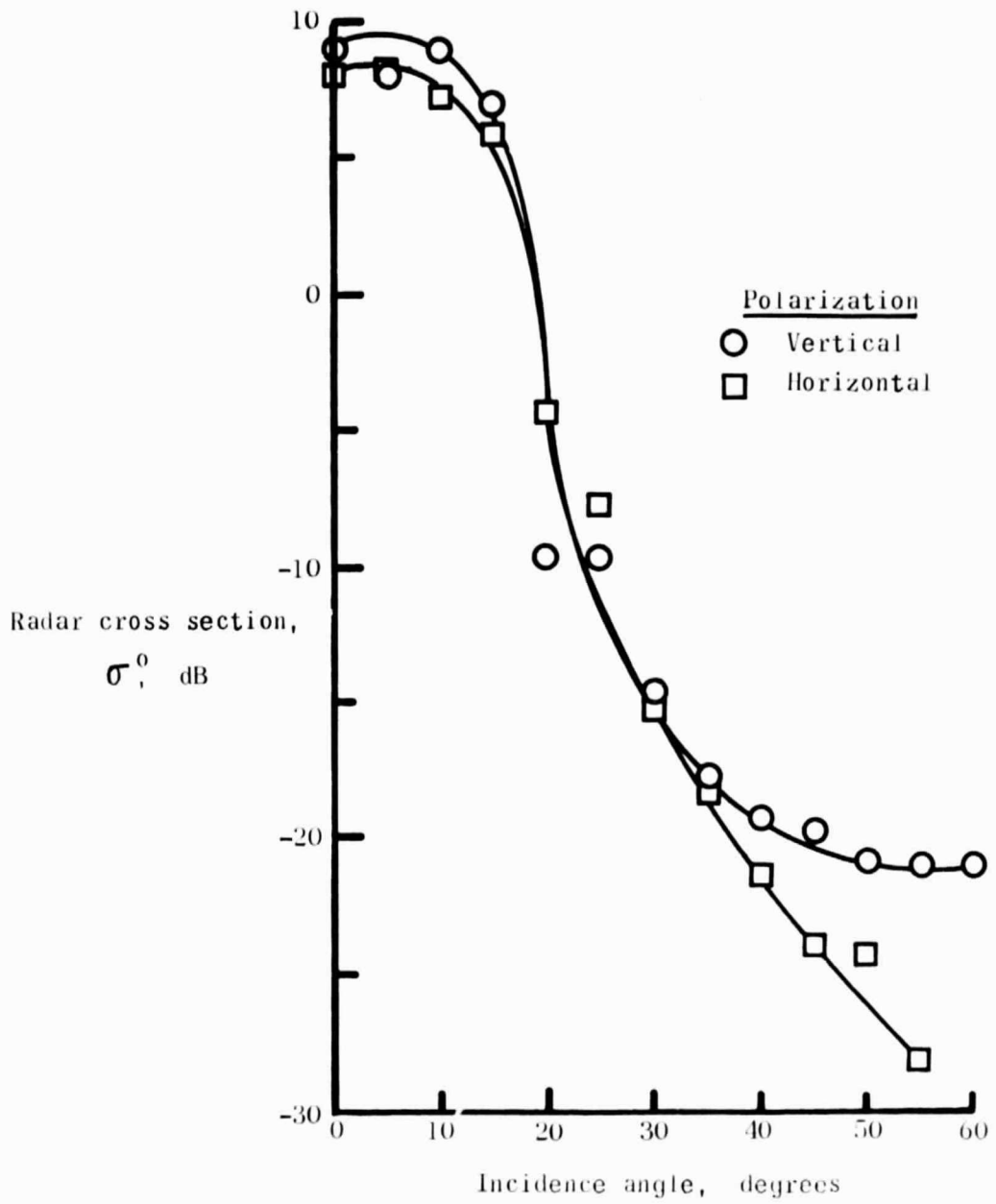

Figure 13.–Normalized radar cross section as a function of viewing angle for wind speed of 4.12 m/sec(8 knots).